# Design, construction and use of a large-sample field-cycled PEDRI imager

David J Lurie, Margaret A Foster, David Yeung† and James M S Hutchison

Department of Biomedical Physics and Bioengineering, University of Aberdeen, Foresterhill, Aberdeen AB25 2ZD, UK

**Abstract.** The design, construction and use of a large-scale field-cycled proton–electron double-resonance imaging (FC-PEDRI) imager is described. The imager is based on a whole-body sized, vertical field, 59 mT permanent magnet. Field cycling is accomplished by the field compensation method, and uses a secondary, resistive magnet with an internal diameter of 52 cm. The magnetic field can be switched from zero to 59 mT or vice versa in 40 ms. It is used with a double-resonance coil assembly (NMR/EPR) comprising a solenoidal NMR transmit/receive coil and a coaxial, external birdcage resonator for EPR irradiation. Experiments to image the distribution of an exogenous nitroxide free radical in anaesthetized rabbits are described.

## 1. Introduction

Proton–electron double-resonance imaging (PEDRI) is a technique for imaging free radicals which is based on the Overhauser effect (also known as dynamic nuclear polarization, DNP). PEDRI was first demonstrated ten years ago (Lurie *et al* 1988), and has been used to study exogenous free radicals in anaesthetized adult rats (Lurie *et al* 1990, Seimenis *et al* 1997), using an imager operating at 10 mT. At this field strength PEDRI cannot be used to image nitroxide free radicals in whole animals larger than rats because of excess power deposition from the EPR irradiation; the technique of field-cycled PEDRI (FC-PEDRI) was developed to counter this problem (Lurie *et al* 1989). In this paper we will describe the design and use of a large-scale FC-PEDRI imager capable of imaging free radicals in animals as large as 2 kg rabbits.

In DNP the NMR resonance of the sample under study is observed in the usual way while an EPR resonance of a free radical solute is irradiated (either continuously or periodically). Under the correct conditions, the EPR irradiation causes a transfer of polarization from the unpaired electrons to the solvent nuclei under study, increasing the intensity of the NMR signal. The enhancement of the NMR signal can be described by the enhancement factor, $E$, given by

$$E = \frac{A_Z}{A_0} \tag{1}$$

where $A_Z$ and $A_0$ are the NMR signals with and without EPR irradiation respectively. The enhancement can be described by the following relationship:

$$E = 1 - \rho f \frac{s}{n} \frac{|\gamma_S|}{\gamma_N} \tag{2}$$

† Present address: Medical Physics Division, Department of Clinical Oncology, Prince of Wales Hospital, 30-32 Ngan Shing Street, Shatin, Hong Kong.

where $\rho$ is the coupling factor ($-1 \leqslant \rho \leqslant \frac{1}{2}$, with $\rho = \frac{1}{2}$ for dipole–dipole interactions), $f$ is the leakage factor ($0 \leqslant f \leqslant 1$), $s$ is the saturation factor ($0 \leqslant s \leqslant 1$), $n$ is the number of hyperfine lines in the EPR spectrum ($n = 3$ for a typical nitroxide free radical) and $\gamma_S$ and $\gamma_N$ are the electron and nuclear gyromagnetic ratios (for experiments involving protons, the ratio $|\gamma_S|/\gamma_N \simeq 659$). Equation (2) assumes that only one EPR resonance is irradiated.

PEDRI involves a combination of DNP with a standard MRI experiment. The DNP effect changes the NMR signal in regions of the sample containing free radical, and these parts exhibit altered signal intensity in the final image. In FC-PEDRI the magnetic field applied to the sample is changed throughout the experiment. The EPR irradiation is applied during the evolution period at low magnetic field strength (at correspondingly low frequency and power), during which the DNP polarization transfer alters the proton magnetization. The magnetic field is then increased rapidly for the detection period, during which the NMR detection pulse(s) and magnetic field gradients are applied. Applying the EPR irradiation at low field decreases the EPR frequency and the power deposition (which goes approximately as the square of the frequency), allowing larger samples to be used. The optimum EPR frequency (and therefore evolution field) depends on the EPR linewidth of the free radical under study and on the size of the sample; it has previously been shown that with nitroxide free radicals and large samples the optimum frequency is between 30 and 60 MHz, corresponding to an evolution field of $\sim$3 mT (Lurie 1994). Detecting the NMR signals at as high a field as possible increases the signal-to-noise ratio (SNR) of the experiment, and hence the sensitivity is increased.

## 2. The large-sample FC-PEDRI apparatus

Figure 1 shows a block diagram of the large-sample FC-PEDRI imager which we have constructed in our laboratory. It is mainly built from commercially available items, but some components were, of necessity, designed and constructed in-house. We will now describe the system components in turn.
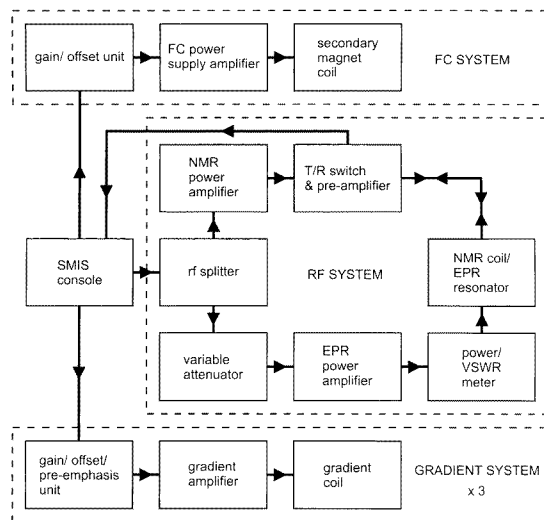


**Figure 1.** Block diagram of the field-cycled PEDRI imager hardware.

## 2.1. Magnet, power supply and gradients

The field compensation method of field cycling is used, with two coaxial magnets (Noack 1986, pp 213–29). The outer, primary magnet operates at a fixed magnetic field $B_0^D$ (the detection field). The inner, secondary magnet generates a magnetic field of variable strength, antiparallel to the primary magnet's field, so that when the secondary magnet is energized the net field at the sample is reduced. The field compensation approach means that the only field present during signal detection is from the constant-field primary magnet, which can be designed with sufficiently good homogeneity for the MRI experiment. The homogeneity of the secondary coil need only be sufficient to cover the EPR resonance linewidth (typically $\sim 100 \ \mu$T) over the volume of interest, and it can therefore be designed for high efficiency and short time constant.

In our imager the primary magnet is a whole-body sized permanent magnet (Field Effects Inc., Acton, MA, USA) with a vertically oriented field of 58.7 mT. It is constructed from magnetized ferrite, has a mass of approximately 2600 kg and a clear bore of 0.65 m. Its homogeneity is approximately 100 ppm over a 30 cm diameter spherical volume (DSV). The supporting structure of the magnet is made from composite materials and, like the ferrite itself, is non-conducting, making it ideal for a field-cycling application since it will not allow eddy currents to flow.

The ferrite magnet has a relatively large temperature coefficient of the magnetic field $(-0.2\% \ ^\circ$C$^{-1})$. The large mass of the magnet results in a very long time constant (of the order of days) for field changes brought about by alterations in ambient temperature, nevertheless it is wise to minimize these effects, and the laboratory is equipped with an air-conditioning unit which maintains the room temperature at $22 \pm 0.5 \ ^\circ$C. Temperature variations within the magnet structure itself are potentially more serious, as they would alter the magnetic field homogeneity in a quasistatic manner; these are prevented by a continuously operating fan which blows room air inside the magnet's thermal cover where it circulates around the ferrite structure.

The secondary magnet is a resistive coil, made from sheets of copper conductor in a saddle configuration. It was designed and constructed by Magnex Scientific Ltd (Abingdon, UK). The coil is wound from copper sheets on a cylindrical former and embedded in epoxy resin. The length of the coil assembly (including the former) is 2 m, the coil itself being 1.5 m in length. Its outer diameter is 64 cm allowing it to fit within the bore of the primary magnet, leaving a free bore of diameter 52 cm. The coil is water cooled on the outer surface of the cylinder, and is equipped with an array of internal platinum resistance thermometers so that its temperature can be continuously monitored during use. It has an inductance of 68 mH and a d.c. resistance of 0.66 $\Omega$, giving it a time constant $(L/R)$ of 103 ms. The magnetic field per unit current is 0.393 mT A$^{-1}$, requiring a current of 149 A to cancel the primary magnet's field. The absolute homogeneity of the magnetic field produced by the secondary coil is approximately $\pm 30 \ \mu$T within a 20 cm DSV at a field offset of 55 mT, sufficient for the nitroxide free radicals which we wish to image. Figure 2 shows a photograph of the complete imager, showing the secondary magnet in place within the primary. Also visible is the partly completed Faraday screen, made from copper foil (40 $\mu$m thickness) on a wooden support. It is important not to make the screen conductor too thick, in order to reduce eddy currents while field cycling. In use, the front face of the screen, with a 67 cm diameter access hole, is fitted in place.

The current for the secondary magnet is generated by a power supply amplifier (Copley Controls Inc., Westwood, MA, USA, model 265P), which is itself powered by two 15 kW d.c. power supplies (Electronic Measurements, Inc., NJ, USA, model ESS 330) operating
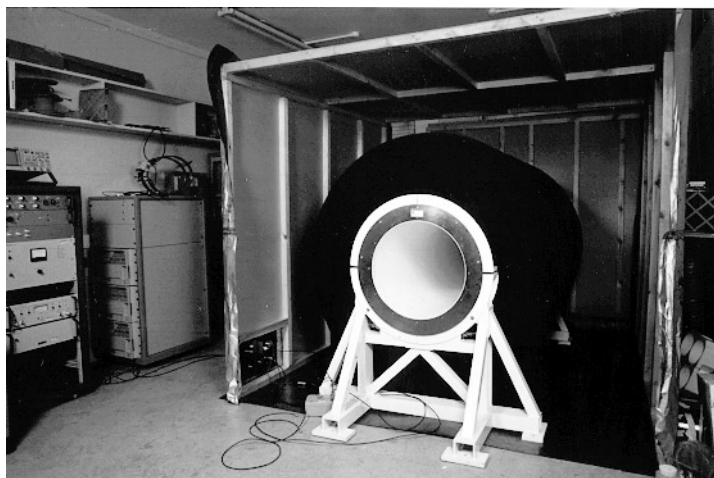
**Figure 2.** Photograph showing the whole-body FC-PEDRI imager, before the Faraday screen was completed. Not seen in the photograph are the RF coil assembly, the secondary magnet power supply and the NMR console.

in parallel. A 0.31 F bank of capacitors is connected across the 330 V output of the d.c. power supplies, in order to supply the necessary current surges during rapid switching of the secondary coil current. The power supply amplifier, d.c. power supplies and capacitor banks are housed in a self-contained 19″ rack assembly. The power supply is able to switch the magnetic field between zero and 58.7 mT (or *vice versa*) in 40 ms.

Conventional bunched-winding gradient coils capable of generating up to 10 mT m$^{-1}$ are built into the structure of the primary magnet. They have low resistance ($\sim$55 m$\Omega$) and high efficiency ($\sim$0.13 mT m$^{-1}$ A$^{-1}$) in order to minimize the thermal load on the permanent magnet. The measured inductances of the coils are 0.55 mH (*X* and *Y*) and 0.67 mH (*Z*). The coils are powered by standard gradient amplifiers (Crown International Inc., IN, USA, model Techron 7794), one per channel.

### 2.2. NMR console

The imager is controlled by a commercially available console (SMIS Ltd, Guildford, UK). This controls all functions of the imager through software running on an integral IBM-compatible PC. The console generates gradient and field-cycling waveforms via four 12-bit digital-to-analogue converters (DACs) which can be programmed independently with arbitrary waveforms. TTL logic waveforms are also generated by the console to enable or disable external modules (RF amplifiers, field cycling amplifier) and these are also programmable by the user. Pulse programs are written in a C-like language and are compiled on the integral PC.

The console also contains a synthesized RF source (Programmed Test Sources Inc., MA, USA, model 310) which provides the RF for the NMR excitation (down-converted to 2.49 MHz) and phase-sensitive detection. As NMR and EPR excitation are never required simultaneously, the same RF source is used to provide the EPR excitation signal (typically 50–200 MHz); switching the frequency between NMR and EPR settings is accomplished under software control.

NMR signals are demodulated within the console and captured by 12-bit analogue-to-digital converters; the sampling rate (and the bandwidth of the anti-alias filters) are software-selectable to values between 1 kHz and 400 kHz (though only 10 kHz was used in this work). Fourier transformation is carried out by a Vector 32C/8500 DSP card under control of the PC; the raw data and magnitude images are saved as separate files. Images are displayed on the PC's monitor, using software supplied with the console.

### 2.3. RF system

NMR excitation pulses generated by the console are sent to a power amplifier (Marconi Ltd., UK, model H1300), then through a passive transmit/receive (T/R) switch (SMIS Ltd, Guildford, UK) to the RF coil. The amplifier has a peak power of 1 kW. NMR signals pass from the RF coil through the T/R switch and are pre-amplified before passing to the console for detection.

EPR irradiation signals generated by the console are amplified by a power amplifier (Kalmus Engineering Inc., WA, USA, model LP400HF) before passing to the EPR resonator through a power meter (RS Components, UK, model W570), which also allows both the forward power and the matching of the resonator to be monitored during an experiment. The EPR RF amplifier has a bandwidth of 5–175 MHz and a peak power of 400 W. At full power the maximum length of pulse is 500 ms with a 10% duty cycle.

The final part of the RF system is the double-resonance RF coil assembly. The NMR transmit/receive coil is a split-solenoid (four + four turns) made from 5 mm diameter copper pipe, with length 14 cm, diameter 14 cm, and an unloaded $Q$-factor of 456. The EPR resonator, which is coaxial with the NMR coil, is an eight-leg, high-pass birdcage resonator tuned to 51 MHz, with length 20 cm, diameter 20 cm, and an unloaded $Q$-factor of 346. The resonator is driven inductively through a coupling loop, and a series trimmer capacitor allows the matching to be adjusted with the sample in place. Interactions between the NMR and EPR coils are minimized by having their RF fields perpendicular. The NMR/EPR coil assembly is housed within a cylindrical RF shield (diameter 30 cm, length 30 cm), made from 40 $\mu$m copper foil.

## 3. Pulse sequences

### 3.1. FC-PEDRI

Figure 3 shows a typical FC-PEDRI pulse sequence, as implemented on our imager. At the start of the pulse sequence the field is ramped down from $B_0^D$ to $B_0^E$ in time $T^{ramp}$. The EPR irradiation is then switched on for time $T^{EPR}$ before the field is ramped back up to $B_0^D$, again in time $T^{ramp}$. There then follows a delay $T^{stab}$ to allow stabilization of the field before the NMR detection RF pulse and associated field gradients are applied. *In vivo* FC-PEDRI images are usually collected using an interleaved version of this pulse sequence, in which the EPR irradiation is only applied during every second evolution period. Alternate NMR signals represent data for 'with EPR' and 'without EPR' images respectively, and the phase-encoding gradient is updated after both signals have been collected. This allows separate 'with EPR' and 'without EPR' images to be collected, and subtraction of the complex data yields a 'difference' image which shows only parts of the sample containing the free radical under study.
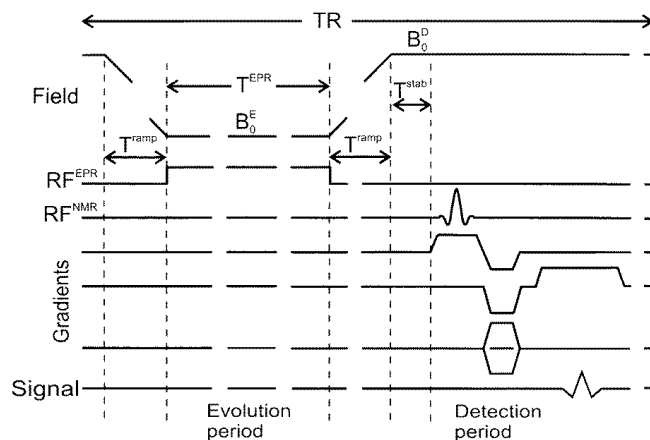
**Figure 3.** FC-PEDRI pulse sequence, showing magnetic field, field gradient and RF waveforms.

### 3.2. FC-DNP

The imager is also used for field-cycled dynamic nuclear polarization (FC-DNP) spectroscopy (Lurie *et al* 1991, Guiberteau and Grucker 1996), using a modified FC-PEDRI pulse sequence in which the selective NMR RF pulse is replaced by a hard pulse, and no gradients are used. Otherwise, the pulse sequence and timing parameters are identical to those in figure 3. In FC-DNP a series of NMR signals are collected using identical EPR irradiation parameters (frequency, power) but with incrementally increasing values of the evolution field $B_0^E$. By plotting NMR signal amplitude against $B_0^E$ an FC-DNP spectrum is displayed, showing the Overhauser-detected EPR resonances of the free radical under study.

## 4. Use of the FC-PEDRI imager

### 4.1. In vivo FC-PEDRI

Female New Zealand White rabbits (about 2.2 kg body weight (b.w.)) were anaesthetized by an intramuscular injection of a ketamine/xylazine mixture (35 mg kg$^{-1}$ b.w. ketamine (Vetalar, Parke-Davis, UK) and 5 mg kg$^{-1}$ xylazine (Rompun, Bayer, UK)). A polythene cannula (0.96 mm outer diameter) was then surgically inserted into the left jugular vein. Once positioned correctly inside the imager a dose of the nitroxide free radical proxyl carboxylic acid (PCA, Sigma Chemical Co.) was administered to the animal through the cannula. The injection solution was made by dissolving PCA, to a concentration of 1.17 M, in bicarbonate buffer. The pH of the injection solution was close to neutral, and it was administered at a dose of 2.27 mM kg$^{-1}$ (approximately 4 ml administered over 2 min). To maintain an appropriate level of anaesthesia throughout the experimental period, extra doses of ketamine/xylazine were given via the cannula, as necessary. After the imaging experiments the animals were killed, under anaesthetic, by an overdose of sodium pentabarbitone (Euthetal, May and Baker, UK) via the cannula.

The procedure for the imaging experiments was as follows: the anaesthetized animal was placed supine inside the NMR/EPR RF coil assembly, with the animal's kidneys placed centrally, and the coil assembly was then placed into the magnet.
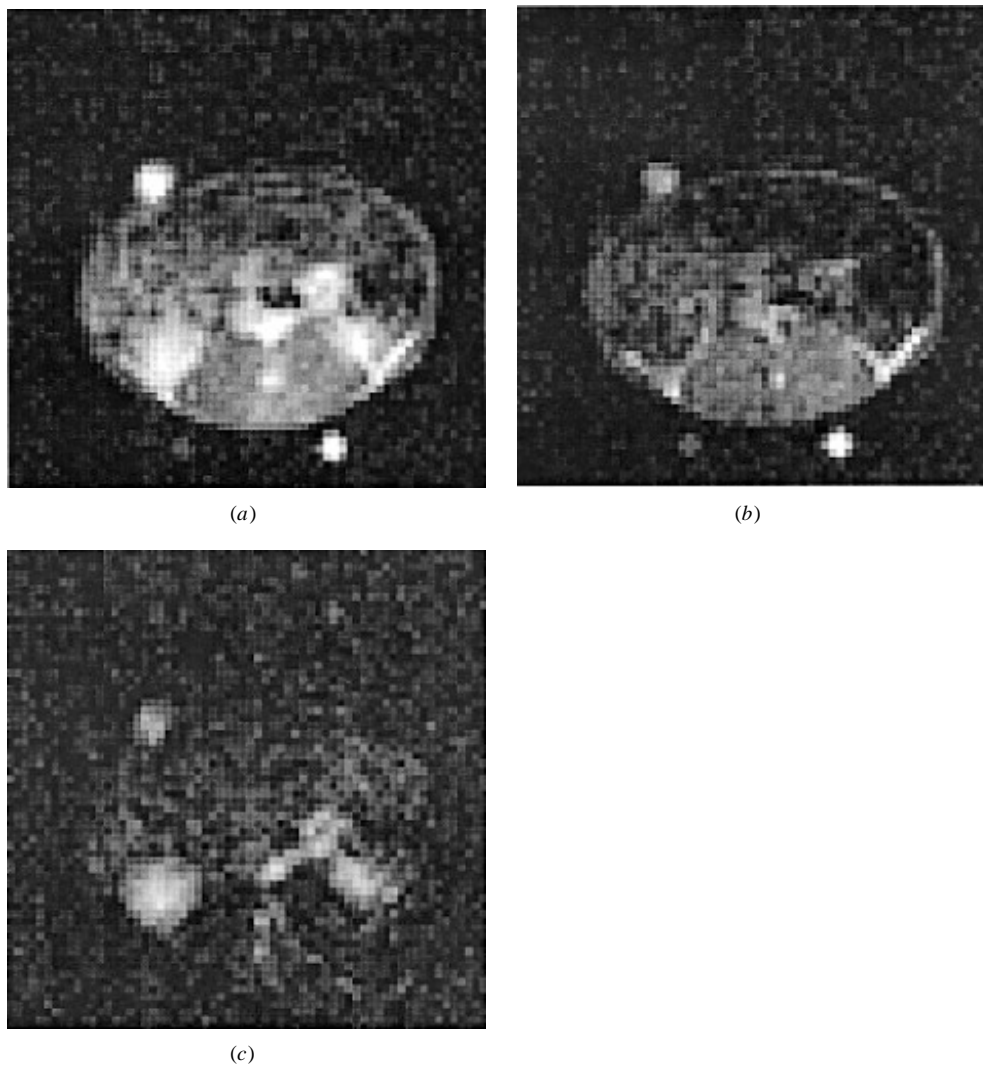
**Figure 4.** Transaxial images through abdomen of anaesthetized rabbit following injection of PCA nitroxide free radical: (*a*) 'without EPR' image, (*b*) 'with EPR' image, (*c*) 'difference' image. The difference image shows the animal's kidneys and major bloodvessels. The high-intensity region above the animal is a reference vial containing 1 mM PCA solution. Vials containing $CuSO_4$ solution are seen below the animal in (*a*) and (*b*); these are used to aid positioning.

The tuning and matching of the birdcage resonator were first checked at low power using a network analyser (Anritsu, Japan, model MS3606B) with a directional coupler (Mini-Circuits, NY, USA, model ZDC-10-1) and adjusted so that the matching was such that the reflected signal was less than $\sim -30$ dB. The resonator was then connected to the EPR power amplifier via the power meter and the pulse sequence was set going in 'set-up' mode using the EPR power and pulse duration chosen for the imaging experiment. The EPR frequency was adjusted in order to minimize the reflected signal, which was monitored using the power meter. This fine adjustment of the EPR frequency was carried out to compensate

for the inevitable change in the birdcage resonator's frequency (typically $-200$ kHz) caused by heating of the resonator's capacitors under high-power operation. Once a steady state was reached, the reflected signal could be maintained at better than $-20$ dB during the experiment, easily sufficient for such a transmit-only experiment.

Once the EPR irradiation parameters had been set up in this way, one or two fixed-field (59 mT) MRI images were collected in order to check the positioning of the animal, after which an interleaved FC-PEDRI image was collected. The nitroxide free radical was then administered, and a series of FC-PEDRI images was obtained, at approximately 6 min intervals.

Images were obtained using both $64 \times 64$ and $128 \times 128$ matrices. In both cases the image parameters were: field-of-view 15 cm, slice thickness 3 cm, $TR = 1000$ ms, $T^{\mathrm{EPR}} = 300$ ms, $T^{\mathrm{ramp}} = 40$ ms, $T^{\mathrm{stab}} = 10$ ms, EPR frequency 51.0 MHz, $B_0^{\mathrm{E}} = 3.05$ mT. The forward power to the birdcage resonator was approximately 300 W, and the power absorbed in the animal can be estimated as 130 W using the loaded and unloaded $Q$ factors (measured to be 193 and 346 respectively). Taking into account the duty cycle of the EPR irradiation (300 ms in 2000 ms, or 15%), the average specific absorption rate (SAR) in a 2.2 kg animal is 9 W kg$^{-1}$. This is higher than desirable, nevertheless the animals were not found to be hyperthermic after two $64 \times 64$ images and two $128 \times 128$ images had been collected over the course of 30 min. Bearing in mind the delays between image collection, the overall SAR was only 3 W kg$^{-1}$.

Figure 4 shows 'without EPR', 'with EPR' and 'difference' transaxial images through the animal's abdomen obtained 2 min after injection of the nitroxide free radical. As in the rat (Seimenis *et al* 1997), PCA is cleared through the rabbit's kidneys, and these can be seen clearly in the difference image, together with major bloodvessels. The signal-to-noise ratio in the difference image is measured to be $14 \pm 1.5$.

### 4.2. FC-DNP

Figure 5 shows an FC-DNP spectrum of a 2 ml, 50 $\mu$M aqueous solution of the nitroxide free radical Tempol (4-hydroxy-2,2,6,6-tetramethylpiperidine-1-oxyl, Sigma Chemical Co.). This spectrum was obtained using a small RF coil assembly tuned to 213 MHz (see figure caption for details). The FC-DNP pulse sequence used had $TR = 1200$ ms and $T^{\mathrm{EPR}} = 400$ ms. As the solution had a $T_1$ of approximately 2.5 s, the sequence timing parameters were by no means optimized ($T^{\mathrm{EPR}}$ should be at least $3T_1$ for the maximum Overhauser effect). Despite this, however, the minimum detectable concentration of Tempol can be estimated from the spectrum to be $\sim 2.5$ $\mu$M under these conditions. It should be noted that the Overhauser effect here causes a $\sim 17\%$ reduction in the NMR signal amplitude at the centre of each Tempol resonance. This is because the low concentration results in a very small value of the leakage factor $f$ (equation (2)), so that

$$\rho f \frac{s}{n} \frac{|\gamma_S|}{\gamma_N} < 1$$

resulting in $0 < E < 1$.

## 5. Conclusions

We have built a field-cycled PEDRI imager with a whole-body sized field-cycling magnet, and have used it to image exogenous free radicals in living rabbits. To our knowledge, this is the first time that free radicals have been imaged in the whole body of any animal larger
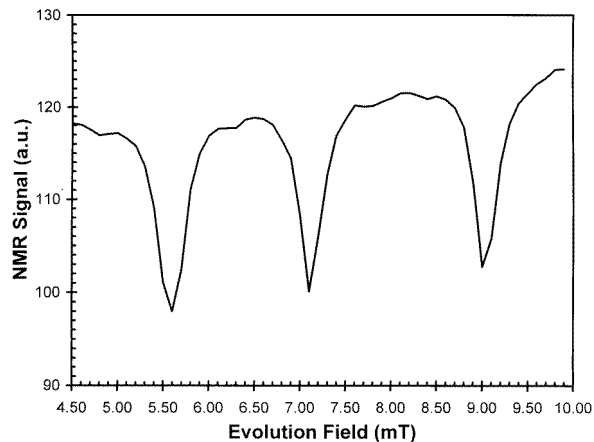
**Figure 5.** FC-DNP spectrum of 2 ml sample of a 50 $\mu$M solution of Tempol free radical. Obtained using a small RF coil assembly, comprising solenoidal NMR coil (length 2.5 cm, diameter 1.6 cm), with coaxial Alderman–Grant resonator (length 4.0 cm, diameter 5.5 cm) (Alderman and Grant 1979). A broadband (1.5–400 MHz) RF amplifier was used for the EPR irradiation (Kalmus Engineering Inc., WA, USA, model 400FC) at 212.7 MHz, incident power $\sim$50 W. Other acquisition parameters: $TR = 1200$ ms, $T^{\text{EPR}} = 400$ ms, $T^{\text{ramp}} = 40$ ms, $T^{\text{stab}} = 20$ ms, evolution field step 0.1 mT.

than a rat, representing an order-of-magnitude increase in sample size. These experiments would not have been possible using fixed-field PEDRI (usually performed at or near 10 mT) because the 237 MHz EPR irradiation would have caused excessive heating of the animal. Although narrow-linewidth free radical probes can potentially be used in large animals at this field strength without excessive heating, field-cycled PEDRI must be used in order to detect and image free radicals with linewidths of 0.1 mT and above. Since this includes most nitroxide free radicals and spin-trapped endogenous radicals, FC-PEDRI is likely to find increasing uses in biomedical research in the coming years.

**Acknowledgments**

**References**

Alderman D W and Grant D M 1979 An efficient decoupler coil design which reduces heating in conductive samples in superconducting spectrometers *J. Magn. Reson.* **36** 447–51
Guiberteau T and Grucker D 1996 EPR spectroscopy by dynamic nuclear polarization in low magnetic field *J. Magn. Reson.* B **110** 47–54
Lurie D J 1994 Progress toward whole-body proton-electron double-resonance imaging of free radicals *Magn. Reson. Mater. Phys. Biol. Med.* **2** 267–71
Lurie D J, Bussell D M, Bell L H and Mallard J R 1988 Proton electron double magnetic resonance imaging of free radical solutions *J. Magn. Reson.* **76** 366–70
Lurie D J, Hutchison J M S, Bell L H, Nicholson I, Bussell D M and Mallard J R 1989 Field-cycled proton-electron double resonance imaging of free radicals in large aqueous samples *J. Magn. Reson.* **84** 431–7

Lurie D J, Nicholson I, Foster M A and Mallard J R 1990 Free radicals imaged *in vivo* in the rat by using proton–electron double-resonance imaging *Phil. Trans. R. Soc.* A **333** 453–6

Lurie D J, Nicholson I and Mallard J R 1991 Low-field EPR measurements by field-cycled dynamic nuclear polarization *J. Magn. Reson.* **95** 405–9

Noack F 1986 NMR field-cycling spectroscopy: principles and applications *Prog. NMR Spectrosc.* **18** 171–276

Seimenis I, Foster M A, Lurie D J, Hutchison J M S, Whiting P H and Payne S 1997 The excretion mechanism of the spin label proxyl carboxylic acid (PCA) from the rat monitored by X-band ESR and PEDRI *Magn. Reson. Med.* **37** 552–8